COMPARISON OF ADVANCED SIGNAL-PROCESSING METHODS FOR ROLLER BEARING FAULTS DETECTION

Jacek Urbanek, Tomasz Barszcz, Tadeusz Uhl

AGH University of Science and Technology, Faculty of mechanical Engineering and robotics, Al. Mickiewicza 30, 30-059 Kraków, Poland
(✉ urbanek@agh.edu.pl, +48 12 617 3116, tbarszcz@agh.edu.pl, thul@agh.edu.pl)

Abstract

Wind turbines are nowadays one of the most promising energy sources. Every year, the amount of energy produced from the wind grows steadily. Investors demand turbine manufacturers to produce bigger, more efficient and robust units. These requirements resulted in fast development of condition-monitoring methods. However, significant sizes and varying operational conditions can make diagnostics of the wind turbines very challenging.

The paper shows the case study of a wind turbine that had suffered a serious rolling element bearing (REB) fault. The authors compare several methods for early detection of symptoms of the failure. The paper compares standard methods based on spectral analysis and a number of novel methods based on narrowband envelope analysis, kurtosis and cyclostationarity approach.

The very important problem of proper configuration of the methods is addressed as well. It is well known that every method requires setting of several parameters. In the industrial practice, configuration should be as standard and simple as possible. The paper discusses configuration parameters of investigated methods and their sensitivity to configuration uncertainties.

Keywords: fault detection, condition monitoring, rolling element bearings, wind turbine.

1. Introduction

In recent years wind energy is the fastest-growing branch of the power generation industry. The distribution of costs during the lifecycle of the unit for wind energy is significantly different from that of traditional, fossil-fired units. First of all, initial investment costs are relatively higher, whereas in traditional units the cost of fuel plays an important role (usually it is the second largest cost). After commissioning, the largest cost for the wind turbine is maintenance. With proper maintenance policies, wind turbines can achieve the highest level of availability in the power generation sector − even up to 98%. The basis of proper maintenance is continuous monitoring of the transmission of the wind turbine. The most successful monitoring methods use vibration signals.

During the last decades, a number of vibration signal-processing techniques have been established. Comprehensive surveys of such techniques are known and can be found in e.g. [1-3]. There are two basic groups of analysis: broadband, and based on selected spectral lines. Basic broadband analysis parameters are:

−   root mean square (RMS);
−   peak-to-peak (P2P);
−   crest factor;
−   kurtosis.

Since they are well-known, a detailed description will be omitted here. Analysis techniques based on selected spectral lines reflect particular frequencies generated by a certain component. Such frequencies are *e.g.*: gear mesh, low shaft harmonics, characteristic bearing harmonics. Due to the different nature of events and to variations in the rotational speed, four basic types of spectra are investigated for the existence of those frequencies:

–   frequency spectrum;
–   order spectrum;
–   envelope spectrum;
–   envelope order spectrum.

Certainly, several more advanced analyses have been developed, but those presented above are implemented in commercial on-line condition monitoring and diagnostics (CM&D). This is caused by the fact that those analyses are easy to understand by a majority of vibration experts, who are rather practice- than theory-oriented. More exhaustive studies on advanced fault detection methods can be found in [4-5, 7], while references [8-9] concentrate directly on condition monitoring of wind turbines. Additional study about character of operation of wind turbines is included in references [10-11].

2. Vibration measurements in wind turbines

Figure 1 [12] presents a typical layout of the wind turbine. The main rotor with three blades is supported by the main bearing and transmits the torque to the planetary gear [13]. The planetary gear input is the plate to which the main rotor is connected. The planetary gear has three planets, with their shafts attached to the plate. The planets roll over the stationary ring and transmit the torque to the sun. The sun shaft is the output of the planetary gear. Further, the sun drives the two-stage parallel gear. The parallel gear has three shafts: the slow shaft connected to the sun shaft, the intermediate shaft and the fast shaft, which drives the generator. The generator produces an AC current of slightly varying frequency. This current is converted first into DC power and then into AC power of frequency equal to the grid frequency. Electric transformations are performed by the controller at the base of the tower. There exist other configurations of wind turbines, where *e.g.* only parallel gear is used. It has typically three stages, to be able to change the rotational speed from ca. 25 rpm on the main rotor to ca. 1500 rpm at the generator.
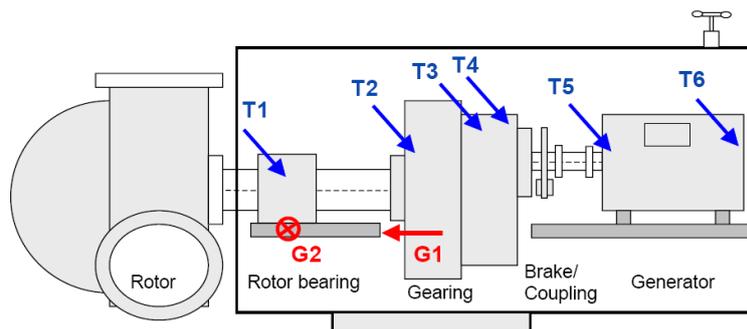

Fig. 1. Typical layout of the wind turbine. Gx and Tx present recommended locations of vibration sensors.

In general, the number of sensors depends on the design of the wind turbine. There are several setups, but the most popular one includes 8 vibration sensors (see Fig. 1). Sensors G1 and G2 are used to monitor structural vibrations of the nacelle and the tower. Sensors T1 … T6 measure vibration of the drive train. On some installations it is possible to combine G1 with T1 and G2 with T2 and only 6 sensors are necessary for monitoring. One of these

www.czasopisma.pan.pl PAN www.journals.pan.pl
POLSKA AKADEMIA NAUK

Metrol. Meas. Syst., Vol. XIX (2012), No. 4, pp. 715-726.

sensors (typically G2/T2) must monitor the transversal direction. T1/G1 measures the axial vibration and all others the vertical one.
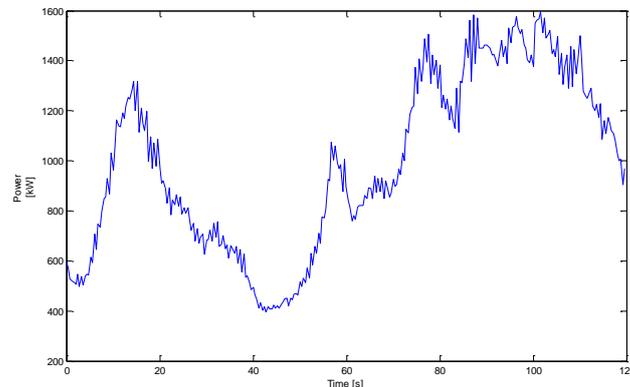

Fig. 2. Changes of generator output power during 120 seconds.

Quick changes of the operational conditions are an important feature of wind turbines [10, 11]. An example of such changes is presented in Fig. 2. During 120 seconds the generator output power varies between 400 and 1400 kW [8]. Such changes have a significant influence on vibration and can blur the changes caused by a malfunction. This is a separate, though very important problem which was discussed *e.g.* in [14].
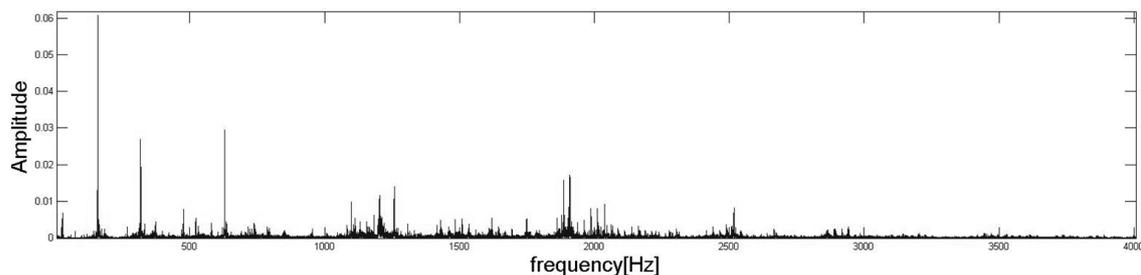

Fig. 3. Fourier spectrum of a typical wind turbine.

The vibration signal from the wind turbine contains mostly gear mesh components with additional shaft components (mostly from the fastest, *i.e.* the generator shaft). As shown in Fig. 3, the spectrum contains components with relatively strong energy up to 3.5 kHz. However, for bearing diagnostics reasons CM&D systems measure vibrations with a 25 kHz sampling frequency, to be able to pick up the structural resonances induced by bearing faults.

3. Case study: rolling element bearing fault

This paragraph presents the case study of a bearing fault in the wind turbine. As mentioned earlier, wind turbines operate under varying operational conditions. Due to constantly changing load, wind turbines are exposed to accelerated wear [15]. Therefore, during a periodical maintenance, the outer race fault on one of bearings was detected using endoscopy. It was the inner race fault on the bearing on the slow shaft of the gearbox (the shaft connecting the planetary gear with the parallel gear). Because of relatively low rotational speed of the investigated shaft, the fault was relatively difficult to detect by typical vibroacoustical methods. Moreover, its signal was masked by another bearing fault, which was located on the generator shaft. A vibration signal generated by faults on the generator shaft can be often recognized even with sensors located on the gearbox due to its high energy.

Such faults are relatively frequent and easy to detect, even with simple envelope-based methods.

Due to the endoscopy investigation, the fault on the slow shaft was too advanced to allow further operation of the turbine. Despite the fact that a CM&D system was installed on the object, it was not able to detect any indicators of the fault. The energy of the characteristic signal component of slowly rotating elements is usually very low and masked by other components and noise. The investigated bearing was mounted on the first stage of the parallel gear, so its ratio in relation to the generator speed was about 1:14.

Both P2P and RMS estimates showed no sensitivity to the fault, even at the final stage of its development. Figs. 4 and 5 present the trend of these analyses for the last 2 years. All further trends in this paper will also cover the same period of time.
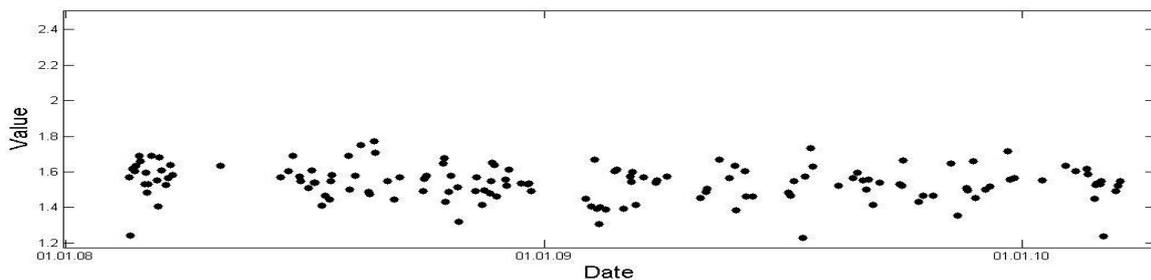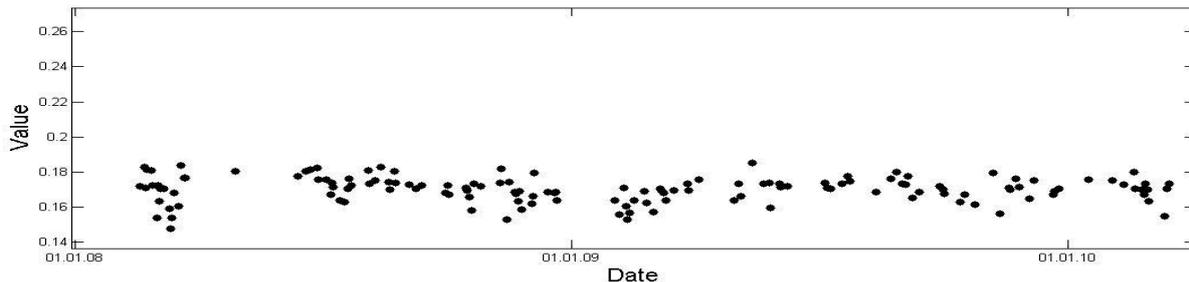

Fig. 4. Trend of PP analysis.

Fig. 5. Trend of RMS analysis.

Such situation is caused by high noise level, large number of other signal components and varying load and speed conditions. Basic time-domain analyses calculated in the wide frequency range are effective only in typical faults of relatively uncomplicated mechanisms operating under steady loads. Thus, it is important to evaluate other, more complex methods.

4. Comparison of fault detection methods

For more effective monitoring frequency-selective methods have to be used. For rolling element bearing monitoring it is common to use the envelope energy as an estimator. However, in the investigated case this method turned out to be inefficient.

Figure 6 presents the energy of the inner race bearing fault frequency component. As presented, no increase can be seen in the trend. The following part of this section will present results of more advanced approaches.
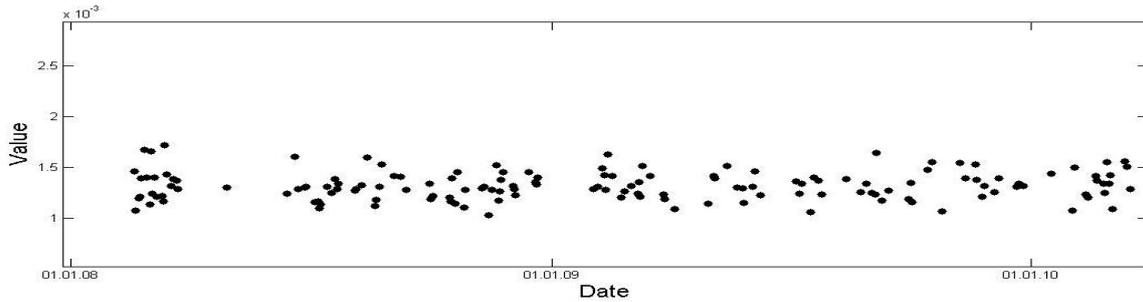
Fig. 6. Component energy calculated from the wideband envelope spectrum.

For effective tracking of bearing fault signatures, it is often fruitful to use the narrow band filtered signal envelope or narrowband envelope analysis (NEA). We actually observe that this method yields best results in many practical cases. The key problem with this approach is the proper selection of the demodulation band.

4.1. Power spectral density difference

To find the proper frequency band for the NEA it is often advisable to compare the spectrum of a signal with fault with that without it. It is a simple method and sometimes can be based only on the signal from the faulty state.

Two signal samples were selected from the database. The first one was from 01.03.2008, from the early days of the CM&D system operation. The second one was recorded during the time period right after endoscopic investigation. Both signals were acquired on the measurement channel closest to the investigated bearing. For clearer results, PSD of both signals were used (see Fig. 7).
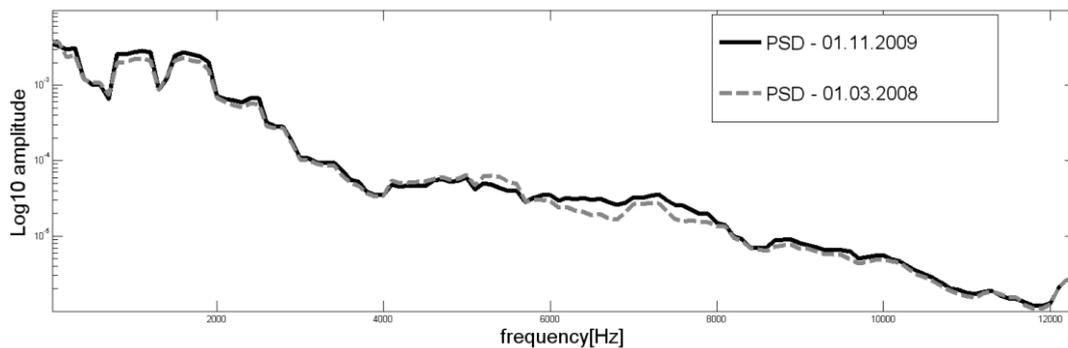

Fig. 7. PSD of the vibration signal from the early operation period (dashed gray line) compared with PSD of a signal from an advanced bearing fault (solid black line). A small increase in PSD can be seen.

A slight increase of the energy can be seen in the frequency band from 6 kHz to 8 kHz. Based on PSD results that band was selected for the demodulation. However, after the narrowband envelope analysis, it turned out that the detected energy growth was caused by development of the generator bearing fault described earlier. Fig. 8 shows the comparison of envelope spectra of both tested signals.
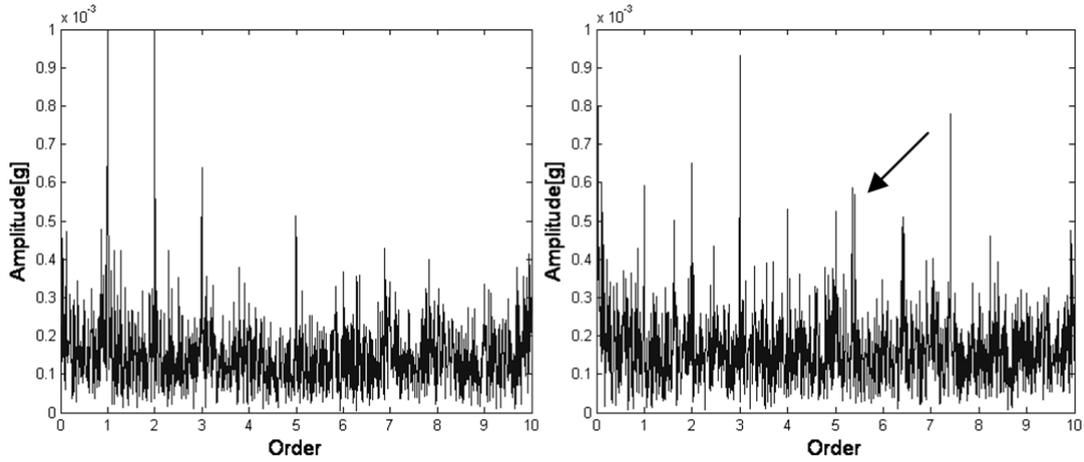
Fig. 8. Narrowband envelope spectra of selected signals. The arrow shows the signature of the generator bearing (not the sought one).

A new strong component can be detected of the order 5.2X, which is the frequency of the generator bearing outer race fault (BPFO). Modulation caused by the strong generator bearing component was effectively masking the low-energy, slow shaft bearing component, which made optimal frequency band selection very difficult. Other methods had to be taken under consideration.

4.2. Kurtogram

First, the authors wanted to propose the Kurtogram [16] analysis as it is a useful method for selecting the optimal frequency band for demodulation. The Kurtogram is a method to present of results of the Spectral Kurtosis (SK) [17-18] analysis. The Spectral Kurtosis is based on the fourth-order spectral cumulant of a conditionally non-stationary process:

$$C_{4Y}(f) = S_{4Y}(f) - 2S_{2Y}^2(f),$$ (1)

where $S_{2nY}(t,f)$ is given by:

$$S_{2nY}(f) = \langle S_{2nY}(t,f) \rangle_t$$ (2)

and can be interpreted as a time-averaged 2nd-order instantaneous moment $S_{2nY}(t,f)$, which is the measure of the energy of the complex envelope and is defined as:

$$S_{2nY}(t,f) = E\left\{ \left| H(t,f)dX(f) \right|^{2n} \big| \omega \right\} / df = \left| H(t,f) \right|^{2n} S_{2nX}.$$ (3)

Thus, the SK is defined as the fourth-order spectral cumulant $S_{4Y}(f)$ normalised by the energy $S_{2Y}^2(f)$, and can be understood as a measure of the peakiness of the probability density function H:

$$K_Y(f) = \frac{C_{4Y}(f)}{S_{2Y}^2(f)} = \frac{S_{4Y}(f)}{S_{2Y}^2(f)} - 2.$$ (4)

The kurtogram was proposed in [16] as a tool for blind identification of detection filters for diagnostics. As a result, a 2-D map (called the kurtogram) is obtained, which presents values of SK calculated for various parameters of frequency and bandwidth. The original kurtogram was based on STFT calculation. A faster version of the kurtogram is the Fast Kurtogram, based on the filterbank approach [5, 16]

Figure 9 presents fast kurtograms of both selected signals. After applying this algorithm to both selected samples, no clear differences were detected.
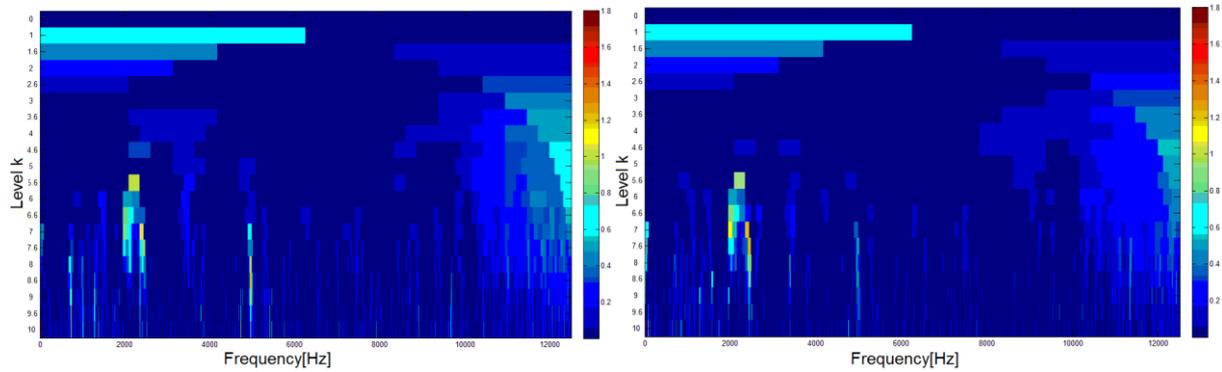

Fig. 9. Kurtogram of a signal with no fault (left) and with advanced bearing faults.

The interpretation of achieved results was difficult, as there were no new modulations in the signal generated by the object operating with a damaged bearing. The envelope spectra were practically identical to the ones from Fig. 8.

4.3. Spectral coherence

Another approach to the problem was the application of a tool based on the analysis of the cyclostationarity properties of the signal. The Spectral Coherence (SCoh) is one of the cyclostationarity signal processing tools and it can represent the dependencies between the modulation (α) and carrier frequencies (f) as a density distribution [4].

The SCoh can be defined as:

$$\gamma_{xx}^{\alpha}(f) = \frac{S_{xx}^{\alpha}(f)}{\sqrt{S_{xx}^{0}(f + \alpha/2)}\sqrt{S_{xx}^{0}(f - \alpha/2)}}, \tag{5}$$

where S_{xx}^{α} is the spectral correlation density (SCD):

$$S_{xx}^{\alpha}(f) = \lim_{\Delta_f \to 0}\lim_{T \to \infty}\frac{1}{T\Delta_f}\int_T x_{\Delta f}(t; f + \alpha/2)x_{\Delta f}^{*}(t; f - \alpha/2)e^{-j2\pi\alpha t}dt. \tag{6}$$

The results of spectral coherence analysis for both tested signals are shown in Fig. 10. The figure was zoomed to the most interesting part.
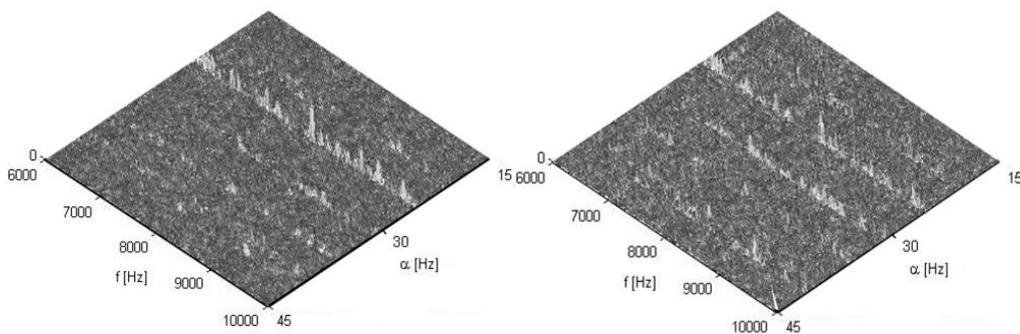

Fig. 10. Spectral coherence of signals: without fault (left) and with fault (right).

It is now clear that the SCoh of the faulty signal does show some differences. The characteristic frequency 31 Hz of the sought gearbox bearing fault is now visible as a modulation signal on the spectral coherence diagram (note that the α frequency increases to the left). There is also a number of components in both plots which shows that the original signal also manifested quite strong cyclostationary behavior. Fig. 10 shows that there is no such thing like "a single resonance". There is rather a range which carries the useful information.
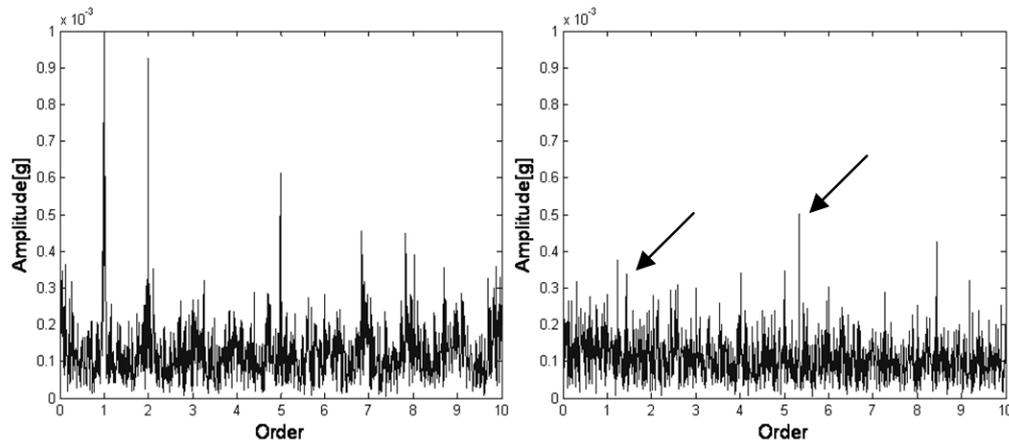

Fig. 11. Narrowband envelope spectra of the signals from Fig. 8. The arrows mark generator bearing fault
(5.2 order) and the sought gearbox bearing fault (1.4 order).

4.4. Improved narrowband envelope analysis

As shown in the previous section, SCoh was able to pick up the fault signature. However, this method is not suited for daily monitoring of a large number of machines. The main reason is the need of processing of 2D SCoh maps. So, the final step of the work was to propose a method which would use advantages of SCoh but return a simplified outcome. Therefore, authors would like to propose NEA with the demodulation band obtained from the SCoh diagram. Based on visual examination of the SCoh results, the optimal frequency band between 8900Hz and 9500Hz was chosen for the signal demodulation as it was a carrier frequencies band containing the majority of modulations of the bearing characteristic frequency sought after. After calculating the envelope spectrum of the signal in the selected frequency range, the energy of a narrowband gearbox bearing characteristic component was used as the fault development indicator. Fig. 12 shows the trend of the proposed analysis.
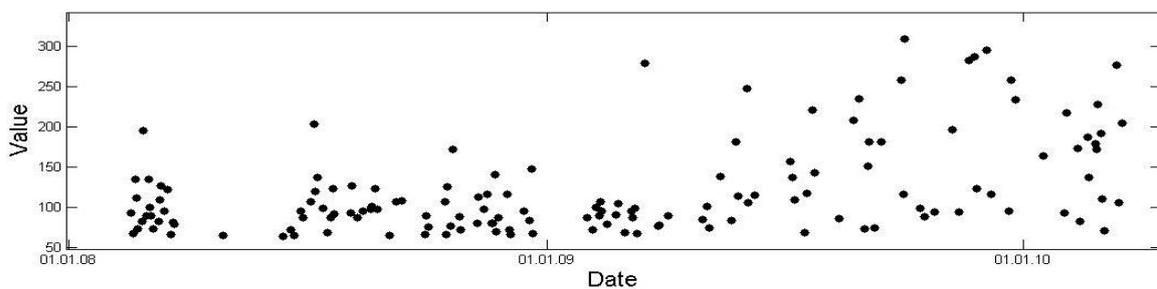

Fig. 12. Trend of energy of the tested bearing characteristic signal.

First indicators of the damage can be recognized around 04.2009, when the level exceeded 250. Results achieved with narrowband envelope analysis were satisfactory but despite that,

authors have also proposed to use kurtosis as a more selective estimator. Fig. 13 shows the trend of kurtosis parameters of the vibration signal demodulated in the same band as for Fig. 12. The important difference between this and the previous analysis is that the first one presents only the energy of the sought component and the second one – the kurtosis resulting from all the components in the assumed frequency band. Therefore, the increase in the kurtosis might be partially due to the other bearing fault and not only to the slowly rotating bearing.
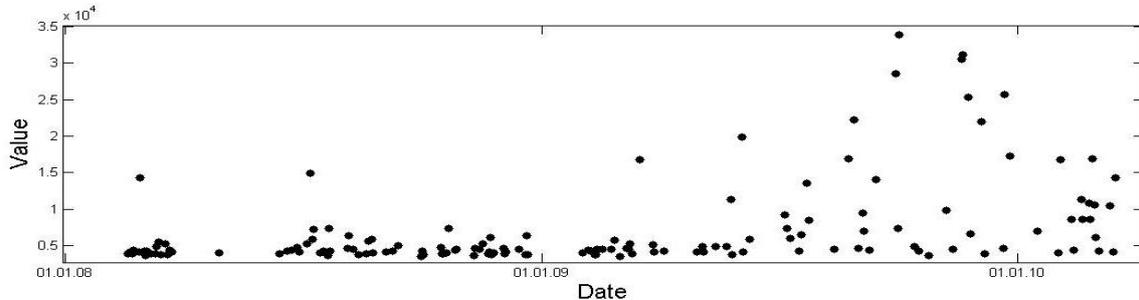

Fig. 13. Trend of kurtosis parameter of the tested bearing characteristic signal frequency range.

The trend in Fig. 13 gave a clearer history of the fault development. In the first step, the increase in the estimator was about 50%, while for the second one it was more than 100% (even including two outliers from the "correct period"). Moreover, around 09.2009 the trend began to decrease. We believe that it was caused by the fact that the local bearing fault started to grow and became an extended fault.

5. Configuration of methods

The previous sections contain the discussion of several estimators which were tested for their applicability to detect a bearing fault on a relatively slow shaft. Apart from actual performance of particular methods, we would like to answer a very important question about the possibility of application of these methods in industrial practice. There are several factors which should be taken into account in such an evaluation. For practical application the method should be relatively easy to configure and it should not be too sensitive to configuration parameters. The complexity of the method is not so important, as modern data processing units becomes more advanced and reliable [19], allowing signal processing tools to be more complex and computationally demanding [20]. Table 1 presents a comparison of the discussed methods.

The first two methods, *i.e.* broadband parameters from raw signal and its envelope, did not detect the fault. On the other hand, these methods are very simple and easy to configure. They can be used as general parameters and might prove themselves useful in the machinery of comparatively uncomplicated kinematics.

The next two methods, narrowband envelope analysis (NEA), coupled with two different ways to determine the demodulation band, hardly detected a fault. The fault signatures were visible, but they were weak compared to other components of the envelope spectrum. This was caused by the existence of another bearing fault on a faster shaft, which gave the other fault relatively high energy. In general, these methods should be useful in practical applications as it is a relatively rare situation for two (or more) separate faults to occur and develop simultaneously. In the single fault cases, it is possible to automatically estimate the optimal frequency band for demodulation.

Table 1. Comparison of bearing fault detection methods.

Method	Detectability	Configuration parameters	Sensitivity to configuration uncertainties	Possibility of simple automated analysis
Broadband parameters of raw signal (RMS, P2P) (Fig. 4 and Fig. 5)	very low	none	low	high
Parameters of broadband envelope (RMS, 2P) (Fig. 6)	low	high pass filter	relatively low	high
NEA + dB difference (Fig. 8)	poor	band pass filter	high	low
Kurtogram (Fig. 9)	poor	band pass filter	high	low
NEA + Spectral Coherence (Fig. 10)	good	band pass filter	high	very low (analysis of 2D maps)
NEA + Spectral Coherence + frequency selective RMS (Fig. 12)	good	band pass filter, band for sought component	high	high
NEA + Spectral Coherence + kurtosis (Fig. 13)	very good	band pass filter, band for sought component	high	high

The method which used the Spectral Coherence for NEA parameters was eventually able to detect the sought fault. However, the analysis of the result was relatively complicated, as it requires processing of the 2-dimentional images. Possible automation of such approach would require an application of comparatively complicated image processing or pattern recognition methods.

The applicability of the SCoh based method was much better, when there was a simple estimator used for the decision making. Out of two such estimators – RMS and kurtosis – the latter has shown higher sensitivity to the fault characteristic component. At this point, it should be stated that configuration of the narrowband envelope analysis methods based on SCoh results requires precise examination of SCoh diagrams, which can make them relatively sensitive to configuration uncertainties.

6. Summary

The paper showed the case study of a wind turbine that had suffered a serious rolling element bearing fault on a relatively low speed shaft. The fault detection was difficult, as there was also a fault in another bearing on the generator shaft, which gave the other fault a stronger signature. The authors have compared several methods for early detection of symptoms of the failure. The paper compares standard methods based on spectral analysis and a number of novel methods based on narrowband envelope analysis, kurtosis and a cyclostationarity approach.

The very important problem of proper configuration of the methods is addressed as well. In industrial practice the configuration should be as standard and simple as possible, so the discussed methods were compared from this perspective. The paper discusses configuration parameters of the investigated methods and their sensitivity to configuration uncertainties.

One has to add that all methods based on the narrowband envelope analysis are very sensitive to the configuration parameters. This is an important problem, especially when one

needs to configure the analysis in hundreds of machines in a short time. There are, however two directions which should simplify this problem. The first one is that in many cases there are only a few machine types (it is the case with wind turbines). We believe that once a demodulation band is determined for a machine, it will be also valid for other machines of the same type. The other direction is research of methods which would return a demodulation band (or another way of obtaining a fault signature) for a given modulating frequency. Such further research could be done especially in the field of cyclostationary methods.

Acknowledgements

References

[1] Zoltowski, B., Cempel, C. (2004). *Engineering of Machinery Diagnostics PTDT ITE PIB Radom*. Warszawa, Bydgoszcz, Radom. (in Polish)

[2] Klein, U., (2003). *Schwingungsdiagnostische Beurteilung von Maschinen und Anlagen (Vibrodiagnostic assessment of machines and devices)*. Stahleisen Verlag, Duesseldorf.

[3] Taylor, T. (2000). *The bearing analysis handbook*. Vibration Consultants Inc.

[4] Antoni, J. (2009). Cyclostationarity by examples. *Mechanical Systems and Signal Processing*, 23, 987-1036.

[5] Randall, R.B., Antoni, J. (2011) Rolling element bearing diagnostics – A. tutorial. *Mechanical Systems and Signal Processing*, 25, 485-520.

[6] Urbanek, J., Antoni, J., Barszcz, T. (2012). Detection of signal component modulations using modulation intensity distribution. *Mechanical Systems and Signal Processing*, 28, 399-413.

[7] Davis, F.B. (1996). *Advanced vibration analysis techniques for fault detection and diagnosis in geared transmission systems. PhD thesis*. Swinburn University of Technology, Australia.

[8] Urbanek, J., Barszcz, T., Zimroz, R., Antoni, J. (2012). Application of averaged instantaneous power spectrum for diagnostics of machinery operating under non-stationary operational conditions. *Measurement* 45, 1782-1791.

[9] Barszcz, T. (2009). Selection of diagnostic algorithms for wind turbines. *Diagnostyka*, 50, 7-12.

[10] Zimroz, R., Barszcz, T., Urbanek, J., Bartelmus, W., Millioz, F., Martin, N. (2011). Measurement Of Instantaneous Shaft Speed By Advanced Vibration Signal Processing – Application To Wind Turbine Gearbox. *Metrol. Meas. Syst.*,18(4), 701-712.

[11] Urbanek, J., Barszcz, T., Sawalhi, N., Randall, R.B. (2011). Comparison of amplitude based and phase based methods for speed tracking in application to wind turbines. *Metrol. Meas.Syst.*, 18(2), 295-304.

[12] Gellermann, T. (2003). *Requirements for Condition Monitoring Systems for Wind Turbines*, *AZT Expertentage*,. Allianz

[13] Hau, E. (2006). *Wind Turbines*. Springer, Berlin.

[14] Zimroz, R, (2009). Some remarks on local damage diagnosis in presence of multi-faults and non-stationary operation. *The Sixth International Conference on Condition Monitoring and Machinery Failure Prevention Technologies*, Dublin, Ireland, The British Institute of Non-Destructive Testing, US Society for Machinery Failure Prevention Technology, 33-44.

[15] Ebner, R., Gruber, P., Ecker, W., Kolednik, O., Krobath, M., Jesner, G. (2010). Fatigue damage mechanisms and damage evolution near cyclically loaded edges. *Bull. Pol. Acad. Sci.-Tech. Sci.*, 58(2).

[16] Antoni, J. (2007). Fast computation of the kurtogram for the detection of transient faults. *Mechanical Systems and Signal Processing*, 21, 108-124.

[17] Antoni, J. (2006). The spectral kurtosis: a useful tool for characterising non-stationary signals. *Mechanical Systems and Signal Processing*, 20, 282-307.

[18] Antoni, J., Randall, R.B. (2006). The spectral kurtosis: application to the vibratory surveillance and diagnostics of rotating machines. *Mechanical Systems and Signal Processing*, 20, 308-331.

[19] Halang, W.A., Śnieżek, M. (2010). A safe programmable electronic system. *Bull. Pol. Acad. Sci.-Tech. Sci.*, 58(3).

[20] Słowik, A. (2011). Application of evolutionary algorithm to design minimal phase digital filters with non-standard amplitude characteristics and finite bit word length. *Bull. Pol. Acad. Sci.-Tech. Sci.*, 59(2).